Journal of the European Ceramic Society 22 (2002) 2827–2833

www.elsevier.com/locate/jeurceramsoc

Mechanical properties of Al_2O_3/ZrO_2 composites

W.H. Tuan*, R.Z. Chen, T.C. Wang, C.H. Cheng, P.S. Kuo

Institute of Materials Science and Engineering, National Taiwan University, Taipei, Taiwan 106, ROC

Received 14 June 2001; received in revised form 28 January 2002; accepted 24 February 2002

Abstract

In the present study, both t-phase zirconia and m-phase zirconia particles are incorporated into an alumina matrix. Dense $Al_2O_3/(t\text{-}ZrO_2 + m\text{-}ZrO_2)$ composites were prepared by sintering pressurelessly at 1600 °C. The microstructure of the composites are characterized, the elastic modulus, strength and toughness determined. Because the ZrO_2 inclusions are close to each other in the Al_2O_3 matrix, the yttrium ion originally in t-ZrO_2 particles can diffuse to nearby m-ZrO_2 particles during sintering, and the m-phase zirconia is thus stabilized after sintering. The strength of the $Al_2O_3/(t\text{-}ZrO_2 + m\text{-}ZrO_2)$ composites after surface grinding can reach values as high as 940 MPa, which is roughly three times that of Al_2O_3 alone. The strengthening effect is contributed by microstructural refinement together with the surface compressive stresses induced by grinding. The toughness of alumina is also enhanced by adding both t-phase and m-phase zirconia, which can reach values as high as two times that of Al_2O_3 alone. The toughening effect is attributed mainly to the zirconia t–m phase transformation.

Keywords: Al_2O_3; ZrO_2; Composites; Strength; Toughness and toughening

1. Introduction

Zirconia has three crystallographic forms, namely: monoclinic (m), tetragonal (t) and cubic (c) phases.[1] The transformation of pure zirconia from t-phase to m-phase occurs at a temperature around 950 °C, which is accompanied by a volume expansion of 4%. This volume expansion generates both dilatational and shear stresses, and these stresses prohibit the opening of an advancing crack, so the toughness of zirconia at room temperature is high compared with other ceramics. In addition to the transformation toughening associated with the t–m transformation around advancing cracks, other mechanisms, such as crack deflection, crack bridging and the presence of microcracks, may also enhance the toughness. Nevertheless, the contribution to toughness from these mechanisms is smaller than that from the transformation toughening.[2] The phase transformation temperature from t to m can be suppressed by doping with suitable alloy elements, such as Y_2O_3, CeO_2, CaO, MgO, etc.[3,4] Furthermore, the size of zirconia particles must be lower than a critical size, to ensure the stable of t-phase at room temperature.[5] Apart from size and composition control, the transformation can also be manipulated by controlling external stresses,[6] external environment,[7] etc. The complexities involved in the phase relationships give many possibilities to design new materials by combining various phases and microstructures.[8]

Zirconia particles are frequently employed as a toughening agent for other ceramics, and these zirconia-toughened ceramics (ZTCs) have received great attention in the last two decades.[2–4] Among these ceramics, many research groups have a very high interest in zirconia-toughened alumina (ZTA), in which either t-phase[3,4] or m-phase[9] zirconia particles were added into alumina. Although the toughness of alumina is indeed enhanced by adopting this approach, the enhancement of toughness may, depending on flaw control or transformation control, be accompanied by a decrease in strength.[9,10] Thus, optimizing the mechanical properties of ZTCs is therefore a long-standing pursuit. In the present study, an alternative design for the composition of ZTA is proposed, where both t-phase and m-phase zirconia particles are added simultaneously into an alumina matrix. The mechanical properties of the $Al_2O_3/(t\text{-}ZrO_2 + m\text{-}ZrO_2)$ composites are investigated.

* Corresponding author. Tel.: +886-2-2365-9800; fax: +886-2-2363-4562.

E-mail address: tuan@ccms.ntu.edu.tw (W.H. Tuan).

0955-2219/02/$ - see front matter
PII: S0955-2219(02)00043-2

2. Experimental procedures

An alumina (TM-DR, Taimei Chem. Co. Ltd., Tokyo, Japan) powder was ball milled together with two ZrO_2 powders (TZ0.5, ZrO_2 + 0 mol% Y_2O_3, d_{50} = 0.3 μm; TZ-3YP, ZrO_2 + 3 mol% Y_2O_3, d_{50} = 0.24 μm, Hanwha Ceramics Co., Australia) in ethyl alcohol for 24 h, using zirconia balls as grinding media. The compositions investigated in the present study are shown in Table 1. The slurry of the powder mixtures was dried with a rotary evaporator, and the dried lumps were crushed and passed through a plastic sieve. Powder compacts with dimensions of 7×6×50 mm were formed by uniaxially pressing at 44 MPa. The sintering was carried out in a box furnace at 1600 °C for 1 h in air with heating and cooling rates of 5 °C/min. For comparison, the Al_2O_3, Al_2O_3/t-ZrO_2 and Al_2O_3/m-ZrO_2 specimens were also prepared with the same techniques. Some discs of 25.4 mm in diameter were prepared for the measurement of elastic modulus with an ultrasonic technique at 5 MHz (Pulser Receiver 5055PR and Oscilloscope 9354CM, LeCoroy Co., USA).

The sintered specimens were machined longitudinally with a 325 grit resin-bonded diamond wheel at a depth of 5 μm/pass. The final dimensions of the specimens were 3×4×36 mm. The strength of the specimens was determined by four-point bending at ambient, room-temperature conditions. The upper and lower spans were 10 and 30 mm, respectively. The rate of loading was 0.5 mm/min. To determine the effect of surface grinding, the strength of some specimens before surface grinding was also determined. The fracture toughness was determined by the single-edge-notched-beam (SENB) technique. The notch was generated by cutting with a diamond saw. The width of the notch was approximately 0.3 mm. No annealing treatment was applied to the notched specimen before the toughness measurement.

Table 1
Composition of the specimens investigated in the present study. The nearest neighbor distance between ZrO_2 particles in Al_2O_3 matrix as calculated by Eq. (1) is also shown

Composition	Total zirconia content (vol.%)	Nearest neighbour distance (μm)
Al_2O_3	0	–
+ 5% t-ZrO_2	5	0.87
+ 7.5% t-ZrO_2	7.5	0.90
+ 10% t-Zro_2	10	0.73
+ 12.5% t-ZrO_2	12.5	0.70
+ 15% t-ZrO_2	15	0.67
+ 5% m-ZrO_2	5	1.6
+ 7.5% m-ZrO_2	7.5	1.4
+ 10% m-ZrO_2	10	1.2
+ 12.5% m-ZrO_2	12.5	1.1
+ 15% m-ZrO_2	15	1.0
+ 5% t-ZrO_2 5% m-ZrO_2	10	1.1
+ 7.5% t-ZrO_2 + 7.5% m-ZrO_2	15	0.92
+ 10% t-ZrO_2 + 10% m-ZrO_2	20	0.87
+ 12.5% t-ZrO_2 + 12.5% m-ZrO_2	25	0.91
+ 15% t-ZrO_2 + 15% m-ZrO_2	30	0.83

Phase identification was performed on sintered, fractured and surface ground surfaces by X-ray diffractometry (XRD) with Cu$K\alpha$ radiation. The relative phase content of zirconia was estimated by using the method proposed by Evans et al.[11] The final density of the specimens was determined by the Archimedes method. The solubility between the materials used in the present study was low; the relative density of the sintered composites was estimated by using the theoretical density of 3.98 g/cm^3 for Al_2O_3, 5.83 g/cm^3 for m-ZrO_2 and 6.05 g/cm^3 for t-ZrO_2. Polished surfaces for microstructure observation were prepared by grinding and polishing with diamond paste to 6 μm and with silica suspension to 0.05 μm. The polished specimens were thermally etched at 1500 °C for 0.5 h to reveal the grain boundaries of matrix grains. Microstructural characterization used scanning electron microscopy (SEM). The size of Al_2O_3 grains and ZrO_2 inclusions was determined by using the line intercept technique. More than 200 grains or inclusions were counted for each specimen.

3. Results and discussion

XRD analysis shows that the initial ZrO_2 powders containing 0 mol% Y_2O_3 and 3 mol% Y_2O_3 are mainly monoclinic and tetragonal phases, respectively; the powders are thus denoted below as m-ZrO_2 and t-ZrO_2 powders.

Table 2 shows the dependence of relative density of Al_2O_3/t-ZrO_2, Al_2O_3/m-ZrO_2 and Al_2O_3/(t-ZrO_2 + m-ZrO_2) composites on total zirconia content. The density values shown in the table are the average value of 8–10 specimens. The density of the composites decreases slightly with the increase of zirconia content, indicating that the presence of zirconia particles prohibits the densification of alumina matrix. Although the solubility of zirconia in alumina is as low as ~2000 ppm, the presence of Zr^{+4} solute can slow down the densification of Al_2O_3.[12] However, the relative density of the specimens, except for the composites with high inclusion content such as 15% t-ZrO_2, 7.5% m-ZrO_2 + 7.5% t-ZrO_2, 15% t-ZrO_2 + 15% m-ZrO_2, is higher than 98%, indicating that the composites can be prepared with straightforward powder mixing and pressureless sintering.

Fig. 1 shows the microstructure of the Al_2O_3/(t-ZrO_2 + m-ZrO_2) composites; and the microstructures of Al_2O_3, Al_2O_3/t-ZrO_2 and Al_2O_3/m-ZrO_2 specimens are also shown for comparison. The zirconia inclusions are distributed uniformly within the composites. The ZrO_2

Table 2
The relative density, size of Al_2O_3 grains, size of ZrO_2 inclusions, the percentage of m-ZrO_2 over total ZrO_2 on the sintered and fracture surfaces of the Al_2O_3/ZrO_2 composites

Composition	Relative density (%)	Size of Al_2O_3 grains (μm)	Size of ZrO_2 inclusions (μm)	m-ZrO_2 on sintered surface (%)	m-ZrO_2 on fracture surface (%)
Al_2O_3	99.7	10.2	–	–	–
+5% t-ZrO_2	99.5	2.1	0.27	~0	4
+7.5% t-ZrO_2	98.2	2.1	0.34	~0	5
+10% t-ZrO_2	99.4	2.0	0.32	~0	6
+12.5% t-ZrO_2	99.4	1.7	0.34	~0	9
-i-15% t-Zr02	97.5	1.5	0.36	~0	10
+5% m-ZrO_2	99.3	3.6	0.50	13	25
+7.5% m-ZrO_2	98.7	2.6	0.53	19	29
+10% m-ZrO_2	99.1	2.4	0.54	22	38
+12.5% m-ZrO_2	99.5	2.4	0.54	26	39
+15% m-ZrO_2	99.4	2.5	0.55	50	22
+5% t-ZrO_2 +5% m-ZrO_2	99.9	1.4	0.49	4	10
+7.5% t-ZrO_2 +7.5% m-ZrO_2	97.3	1.6	0.49	4	12
+10% t-ZrO_2 +10% m-ZrO_2	99.9	1.2	0.54	6	11
+12.5%t-ZrO2+ 12.5% m-ZrO_2	99.7	1.2	0.63	8	13
+15% t-ZrO_2 +15% m-ZrO_2	96.1	1.0	0.63	32	10

particles, both t-phase and m-phase, are mainly located at the grain boundaries of alumina, so the microstructure of alumina is thus refined due to the pinning effect exerted by the zirconia particles, as shown in Table 2. The size of alumina grains in the t-ZrO_2-containing composites is smaller than that in the Al_2O_3/m-ZrO_2 composites, indicating that the presence of a small amount of Y_2O_3, the stabilizing agent for ZrO_2, can further prohibit the grain growth of alumina. Though the ionic charge of yttrium is the same as that of

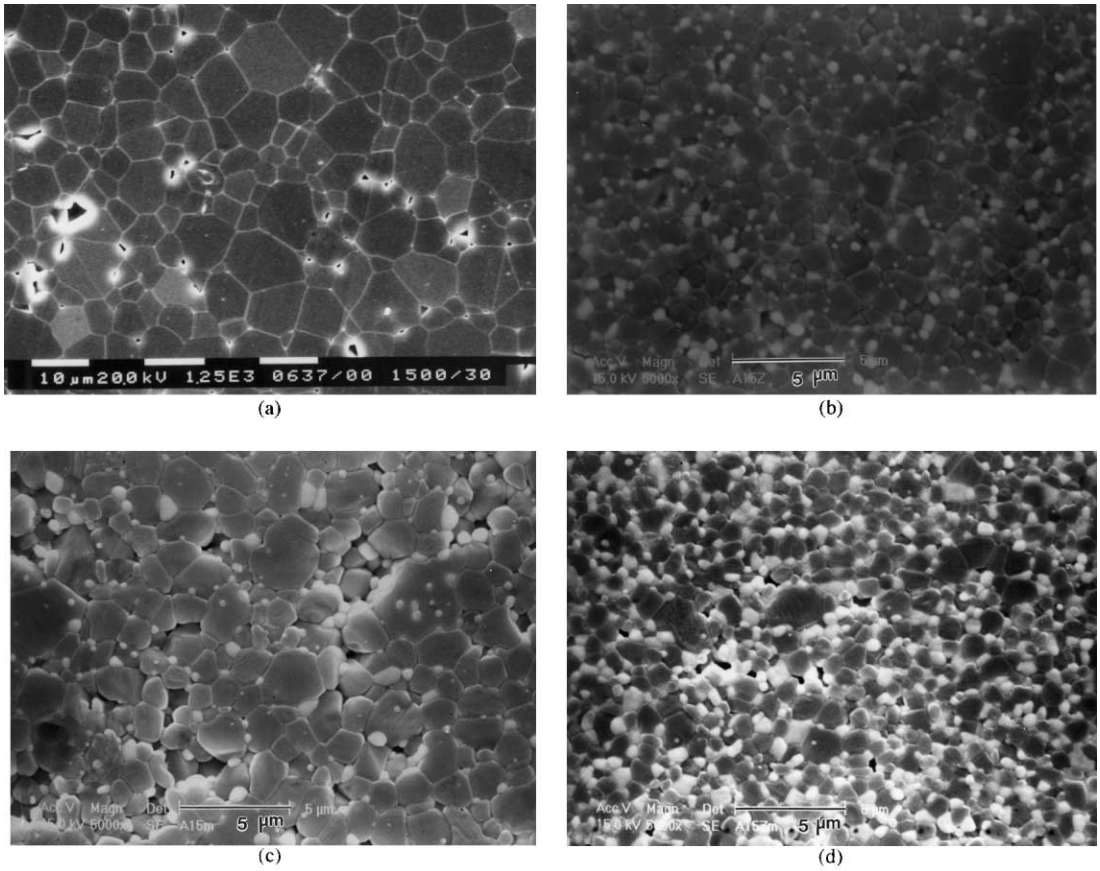

Fig. 1. Microstructures of (a) Al_2O_3, (b) Al_2O_3/15% t-ZrO_2, (c) Al_2O_3/15% m-ZrO_2 and (d) Al_2O_3/(15% t-ZrO_2+15% m-ZrO_2) composites.

aluminum, the yttrium ion is much larger than the aluminum ion (0.89 angstrom vs. 0.53 angstrom).[13] Large yttrium ions tend to segregate at the grain boundaries of alumina, thus reducing elastic strain energy.[14] Although the solubility of yttrium in alumina is extremely low (<10 ppm),[15] large yttrium ions can block the diffusion of ions along grain boundaries, leading to reduced densification and grain growth rates.[16] Though the yttria content in the composites is low, the amount is high enough to suppress the coarsening of alumina matrix grains.

Table 2 also shows the size of zirconia particles of the Al_2O_3/ZrO_2 composites. The ZrO_2 inclusions grow to a size that is roughly two times that of the starting particle size after sintering. The size of ZrO_2 inclusions in the sintered Al_2O_3/m-ZrO_2 composites is larger than that in the sintered Al_2O_3/t-ZrO_2 composites. The grain growth of zirconia in alumina matrix is a process of coalescence; namely, the coarsening of zirconia particles is accompanied by the grain growth of alumina matrix.[17] The size of Al_2O_3 grains in Al_2O_3/m-ZrO_2 composites is larger than that in Al_2O_3/t-ZrO_2 composites, so the ZrO_2 inclusions in Al_2O_3/m-ZrO_2 composites are thus larger than those in Al_2O_3/t-ZrO_2 composites. For the Al_2O_3/(t-ZrO_2 + m-ZrO_2) composites, no attempt is given to distinguish the phase of each ZrO_2 particle. The value shown for the ZrO_2 inclusions in the Al_2O_3/(t-ZrO_2 + m-ZrO_2) composites in Table 2 is the average size for all ZrO_2 inclusions. The size of ZrO_2 inclusions in the Al_2O_3/(t-ZrO_2 + m-ZrO_2) system is between the other two systems. Some fine ZrO_2 particles in the Al_2O_3/m-ZrO_2 composite are trapped into Al_2O_3 matrix grains, Fig. 3(c), perhaps due to the relatively greater grain growth of the alumina matrix.

Table 2 shows the amount of m-ZrO_2 on the surface of the sintered composites. The amount of m-ZrO_2 on the surface of Al_2O_3/m-ZrO_2 composites is the highest, on the Al_2O_3/t-ZrO_2 composites the lowest, on the Al_2O_3/(t-ZrO_2 + m-ZrO_2) composites in the intermediate. The presence of Y_2O_3 lowers the transformation temperature from t to m down to a temperature below room temperature,[2] so less m-phase is detected in the t-ZrO_2 containing systems. Though less constraint is imposed on zirconia particles near the surface region, there is hardly any m-phase detected on the sintered Al_2O_3/t-ZrO_2 composite. Even though m-ZrO_2 particles are used as the starting material for the Al_2O_3/m-ZrO_2 composites, only part of the ZrO_2 particles transform to m-phase, indicating that after sintering some ZrO_2 particles remain at its high-temperature phase as metastable t-phase. The elastic modulus of pure alumina is high, 396 GPa, as determined by the ultrasonic technique. The rigid Al_2O_3 matrix constraints the fine ZrO_2 inclusions, thus suppressing the extent of phase transformation. Furthermore, the size of ZrO_2 particles in the Al_2O_3/m-ZrO_2 composites is larger than that of ZrO_2 particles in the other two systems. Many ZrO_2 particles can thus be larger than the critical size for the transformtion,[5] so more m-phase is thus detected in the Al_2O_3/m-ZrO_2 composites.

The amount of m-phase is also very low, $\sim$4%, on the surface of the sintered Al_2O_3/(t-ZrO_2 + m-ZrO_2) composites, as shown in Table 2. For a composite containing monosized inclusions, the nearest neighbor distance, λ, between inclusions depends on the size of inclusion, d, and its volume fraction, F, as[18,19]

$$\lambda = \left(\frac{\pi}{6}\right)^{1/2} \frac{d}{F^{1/2}} \quad (1)$$

The calculated values for the distance between nearest neighboring ZrO_2 particles in Al_2O_3 matrix are shown in Table 1. The diffusion coefficient of yttrium ion in alumina is not available from the literature. However, the distance between ZrO_2 particles is so small that the transportation of yttrium ions from t-ZrO_2 to nearby m-ZrO_2 particles is thus possible. The m-ZrO_2 particles are stabilized after the adsorption of Y_2O_3 from the nearby t-ZrO_2 particles. Therefore, the amount of m-

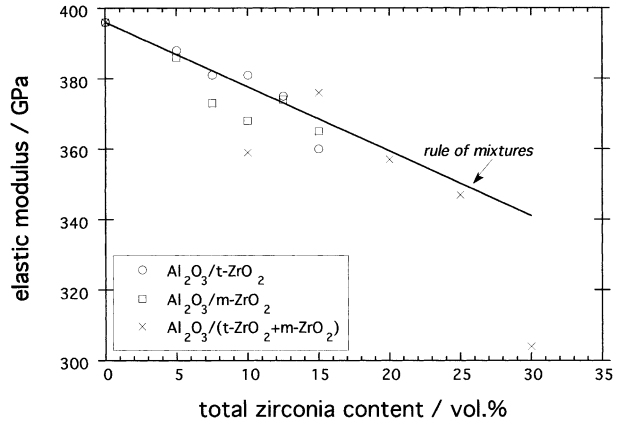

Fig. 2. Elastic modulus of composites as function of total zirconia content. The straight line predicted by the rule of mixtures is shown for comparison.

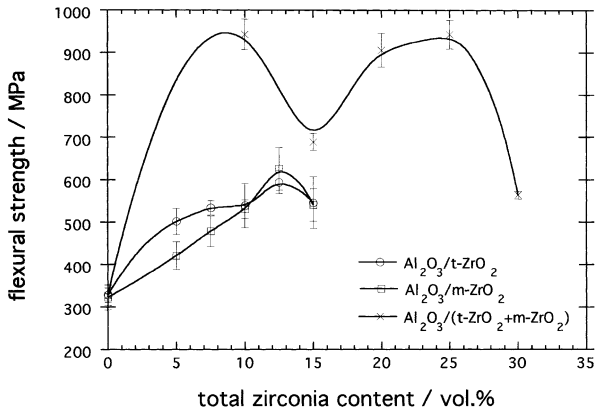

Fig. 3. Flexural strength of composites as a function of total zirconia content.

phase in the sintered $Al_2O_3/(t\text{-}ZrO_2 + m\text{-}ZrO_2)$ composites is lower than that in the $Al_2O_3/m\text{-}ZrO_2$ composite, even though the same amount of m-ZrO_2 was used in the starting compositions.

Fig. 2 shows the elastic modulus of the composites as a function of total zirconia content. The values calculated from the rule of mixtures are also shown in the figure for comparison. The elastic modulus of zirconia, 200 GPa,[20] is lower than that of alumina; thus the elastic modulus decreases with the increase of zirconia content. As-sintered specimens, without surface grinding, were used for the elastic modulus measurement. The ultrasonic wave penetrates through the specimens, unlike the XRD analysis, which detects only the region near the surface. The elastic modulus measurement can thus provide more information for the interior of the composites. The presence of porosity and microcracks can reduce the elastic modulus. The densities of the composites with low zirconia content (<10 vol.%) are almost equal (Fig. 2); however, the elastic modulus of the $Al_2O_3/m\text{-}ZrO_2$ composites is slightly lower than that of the $Al_2O_3/t\text{-}ZrO_2$ composites and of the values predicted by the rule of mixtures, suggesting the possibility of the presence of a small amount of microcracks in the $Al_2O_3/m\text{-}ZrO_2$ composites. The density of $Al_2O_3/(15\%t\text{-}ZrO_2 + 15\%m\text{-}ZrO_2)$ composite is the lowest of the composites, whereas it has the largest zirconia inclusions, so some microcracks may be present in the composite. Thus the elastic modulus of this composite is the lowest.

Fig. 3 shows the strength of the composites as a function of total zirconia content. The presence of either or both t-ZrO_2 and m-ZrO_2 refines the microstructure of alumina matrix, as shown in Table 2. The strengthening effect is partly attributed to the refinement of microstructure. The strength of the $Al_2O_3/(t\text{-}ZrO_2 + m\text{-}ZrO_2)$ system is the highest among the three systems, reaching 940 MPa. The low density of $Al_2O_3/(7.5\%$ t-$ZrO_2 + 7.5\%$ m-$ZrO_2)$ and $Al_2O_3/(15\%$ t-$ZrO_2 + 15\%$ m-$ZrO_2)$ composites, Table 2, underlines their low strength. The size of matrix grains in the $Al_2O_3/(t\text{-}ZrO_2 + m\text{-}ZrO_2)$ composites is reduced to 1/5 that of Al_2O_3 alone, Table 2. The strength of ceramics is inversely proportional to the square root of the grain size;[21] however, the strength of $Al_2O_3/(t\text{-}ZrO_2 + m\text{-}ZrO_2)$ composites is nearly three times that of Al_2O_3 alone. The microstructural refinement alone is not sufficient to account for such strength enhancement. The strength of the Al_2O_3, $Al_2O_3/5\%$ t-ZrO_2, $Al_2O_3/5\%$ m-ZrO_2 and $Al_2O_3/(5\%$ t-$ZrO_2 + 5\%$ m-$ZrO_2)$ specimens before and after surface grinding is shown in Table 3. The strength of Al_2O_3 specimens increases by 20% after the surface grinding treatment. The strength of a brittle solid depends on the size of its critical flaws and the surface grinding process can alter the size of critical flaws and introduce compressive stresses into surface layer.[22] The population of flaws tends to be higher near surface region because contamination is easily introduced into the surface region during various processing steps. The strength is thus enhanced because the surface region is removed after grinding. In addition to the surface modification, residual compressive stress is also introduced into the surface layer by grinding, and the residual compressive stress can also contribute to increased strength.

The strength of $Al_2O_3/5\%$ t-ZrO_2, $Al_2O_3/5\%$ m-ZrO_2 and $Al_2O_3/(5\%$ t-$ZrO_2 + 5\%$ m-$ZrO_2)$ composites increases by 60, 40 and 120% after surface grinding, respectively. There are approximately 3% ZrO_2 particles transformed from t to m phase in the surface region of the machined $Al_2O_3/5\%$ t-ZrO_2 composite as shown in Table 3. The expansion of ZrO_2 particles during t–m transformation can further introduce compressive stresses into the surface layer, so the strength of $Al_2O_3/t\text{-}ZrO_2$ composites is therefore enhanced.

The critical transformation stress from t to m-phase increases with the increase of Y_2O_3 content.[23] The stresses, shear and tensile stresses, applied by the diamond wheel during grinding seems too small to trigger a significant amount of phase transformation of ZrO_2 particles in $Al_2O_3/t\text{-}ZrO_2$ (3 mol% Y_2O_3) composite (Table 3). The effective Y_2O_3 content in ZrO_2 particles in the $Al_2O_3/(t\text{-}ZrO_2 + m\text{-}ZrO_2)$ composites is lower than 3 mol%, so the ZrO_2 particles are thus easier to transform. Therefore, 16% of the ZrO_2 particles transform to m-phase. Consequently, the strength of the machined $Al_2O_3/(5\%$ t-$ZrO_2 + 5\%$ m-$ZrO_2)$ composite is twice that of the composite before grinding. The

Table 3
The strength of the Al_2O_3, $Al_2O_3/5\%$ t-ZrO_2, $Al_2O_3/5\%$ m-ZrO_2 and $Al_2O_3/(5\%$ t-$ZrO_2 + 5\%$ m-$ZrO_2)$ specimens before and after surface grinding. The percentage of the phase transformation on the surface before and after grinding is also shown

	Strength/MPa		Extent of phase transformation/%	
	As-sintered	After surface grinding	As-sintered	After surface grinding
Al_2O_3	269±18	323±30	–	–
$Al_2O_3/5\%$ t-ZrO_2	310±25	502±31	~0	~3
$Al_2O_3/5\%$ m-ZrO_2	303±23	421±33	13	34
$Al_2O_3/(5\%$ t-ZrO_2 + 5% m-$ZlO_2)$	424±46	926±67	~4	16

amount of m-phase zirconia is high, 34%, on the surface of the machined Al_2O_3/5% m-ZrO_2 composite. The amount of transformation may be too high to produce some interconnected microcracks after phase transformation, and the strength increase is thus limited by the excess transformation.

Fig. 4 shows the dependence of toughness of the composites on total zirconia content. The toughness of the Al_2O_3/m-ZrO_2 composites is the highest among three systems, reaching 11.8 MPam$^{0.5}$. The amount of m-phase on the fracture surface of the Al_2O_3/t-ZrO_2 composites is very low, as shown in Table 2. For Al_2O_3/m-ZrO_2 composites, more m-phase can be detected on the fracture surface, indicating more phase transformation participating in the fracture process. The amount of m-phase on the fracture surface of Al_2O_3/(t-ZrO_2 + m-ZrO_2) composites is also low, suggesting that m-ZrO_2 particles are stabilized, or metastable, due to the supply of Y_2O_3 from nearby t-ZrO_2 particles. Fig. 5 shows the toughness as a function of percentage of phase transformation. Hannink et al.[2] suggested that the toughness could increase linearly with the amount of transformable zirconia, provided the transformation toughening dominates during fracture. Such a linear relationship is indeed exhibited in the systems investigated in the present study. Fig. 5 demonstrates that the toughness enhancement for all the composites investigated in the present study can be attributed mostly to a transformation toughening effect. The contribution from other toughening mechanisms, such as microcracking, crack deflection, is small. The toughness of the composites thus depends strongly on the extent of phase transformation. The toughness of the Al_2O_3/m-ZrO_2 composites, where no stabilizing agent is added to the ZrO_2, is thus the highest among three systems.

Fig. 6 presents all the toughness and strength data for the composites, showing that the strength of composites increases with the increase of toughness. However, the strength of Al_2O_3/m-ZrO_2 composites is significantly lower than that of Al_2O_3/t-ZrO_2 and of Al_2O_3/(t-ZrO_2 + m-ZrO_2) composites in terms of toughness. A small amount of microcracks may exist in the Al_2O_3/m-ZrO_2 composites, as demonstrated by the elastic modulus analysis (Fig. 2). The strength thus suffered due to the presence of microcracks.

Though the toughness of Al_2O_3/(t-ZrO_2 + m-ZrO_2) composites ranges between those of Al_2O_3/t-ZrO_2 and Al_2O_3/m-ZrO_2 composites, its strength is the highest among all three systems. For example, the strength and toughness of Al_2O_3/(5% t-ZrO_2 + 5% m-ZrO_2) composites is 943 MPa and 7.2 MPam$^{0.5}$, respectively. The total zirconia content for the composite is only 10%; the strength and toughness are respectively, three and two times that of alumina alone. There was 3 mol% Y_2O_3 in the t-ZrO_2 particles in the beginning, and Y_2O_3 can diffuse from t-ZrO_2 particles to m-ZrO_2 particles during the sintering of Al_2O_3/(t-ZrO_2 + m-ZrO_2) composites. The final effective Y_2O_3 content in the ZrO_2 particles may be in the range of 1–2 mol%. These ZrO_2 particles transform easier under external stress, so a residual compressive stress is thus introduced into the surface region during grinding, and the strength is thus enhanced significantly. Many zirconia powders are

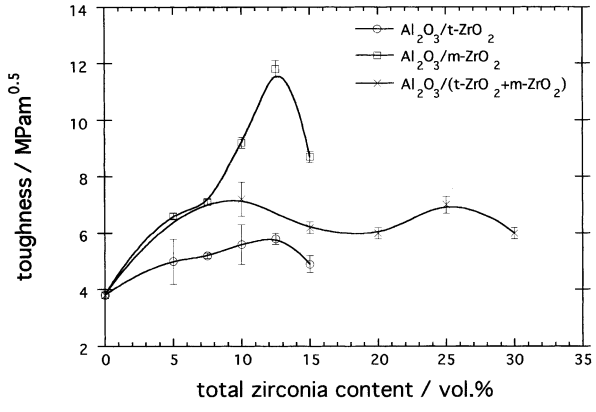

Fig. 4. Toughness of composites as a function of total zirconia content.

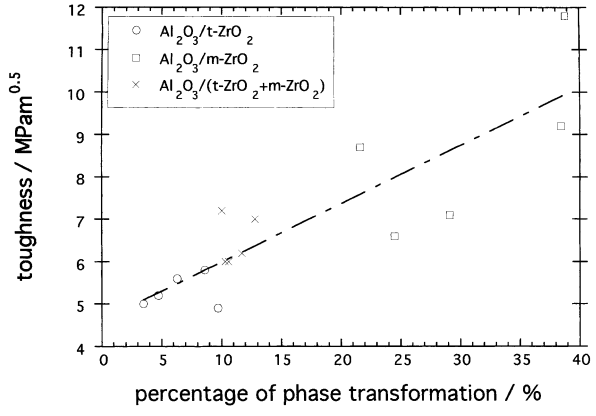

Fig. 5. Toughness of composites as a function of the percentage of phase transformation.

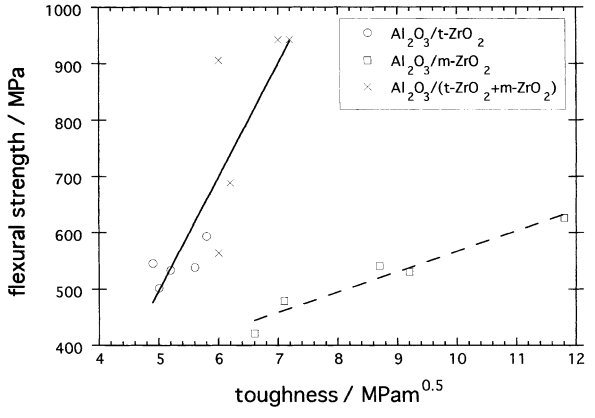

Fig. 6. Strength of composites as a function of toughness.

available on the market; however, these are mainly 0 or 3 mol% Y_2O_3 powders. The present study demonstrates that the amount of Y_2O_3 dopant can be easily manipulated by mixing various amounts of t-phase and m-phase powders together. The approach adopted in the present study provides an alternative to design Al_2O_3/ZrO_2 composites with improved mechanical properties.

4. Conclusions

The present study demonstrates that adding both t-ZrO_2 and m-ZrO_2 particles can significantly enhance the mechanical properties of alumina. The presence of Y_2O_3, originally in the t-ZrO_2 particles, can affect the microstructural evolution of Al_2O_3 matrix and the phase transformation of ZrO_2. The m-ZrO_2 phase is stabilized due to the adsorption of yttria from nearby t-ZrO_2 phase. Fewer zirconia inclusions are transformed from t to m in the Al_2O_3/(t-ZrO_2 + m-ZrO_2) composites than in the Al_2O_3/m-ZrO_2 composites. A compressive surface layer is formed on the machined surface due to the volume expansion accompanied by the t–m transformation. The strength can thus be enhanced due to the microstructural refinement and the presence of the surface stresses. The toughness enhancement is proportional to the amount of transformable zirconia, indicating that the toughening effect is mainly contributed by a transformation toughening effect.

Acknowledgements

The National Science Council, R.O.C. supported the present study through contract number NSC89–2216-E002–049.

References

1. Subbarao, E. C., Zirconia—an overview. In *Advances in Ceramics*, ed. A. H. Heuer and L. W. Hobbs. Am. Ceram. Soc. Inc., OH, USA, 1981, pp. 1–24.
2. Hannink, R. H. J., Kelly, P. M. and Muddle, B. C., Transformation toughening in zirconia-containing ceramics. *J. Am. Ceram. Soc.*, 2000, **83**, 461–487.
3. Heuer, A. H. and Hobbs, L. W., ed., *Advances in Ceramics,* Vol. 3. Am. Ceram. Soc. Inc., OH, USA, 1981.
4. Claussen, N., Ruehle, M. and Heuer, A. H., ed., *Advances in Ceramics,* Vol. 12. Am. Ceram. Soc, Inc., OH, USA, 1984.
5. Garvie, R. C., Critical size effects in alumina–zirconia alloys. In *Advances in Ceramics*, ed. N. Claussen, M. Ruhle and A. H. Heuer. Am. Ceram. Soc., Columbus, USA, 1988, pp. 55–69.
6. Ruehle, M. and Evans, A. G., High toughness ceramics and ceramic composites. *Prog. Mater. Sci.*, 1989, **33**, 85–167.
7. Hirano, M., Inhibition of low temperature degradation of tetragonal zirconia ceramics—a review. *Br. Ceram. Trans. J.*, 1992, **91**, 139–147.
8. Claussen, N., Microstructural design of zirconia-toughened ceramics (ZTC). In *Advances in Ceramics*, ed. N. Claussen, M. Ruhle and A. H. Heuer. Am. Ceram. Soc., Columbus, USA, 1984, pp. 325–351.
9. Claussen, N., Steeb, J. and Fabst, R. F., Effect of induced microcracking on the fracture toughness of ceramics. *Am. Ceram. Soc. Bull.*, 1977, **56**, 559–562.
10. Swain, M. V., Inelastic deformation of Mg-PSZ and its significance for strength-toughness relationship of zirconia toughened ceramics. *Acta Metall.*, 1985, **33**, 2083–2091.
11. Evans, P. A., Stevens, R. and Binner, J. P., Quantitative X-ray diffraction analysis of polymorphic mixes of pure zirconia. *Br. Ceram. Trans. J.*, 1984, **84**, 39–43.
12. Majumdar, R., Gilbart, E. and Brook, R. J., Kinetics of densification of alumina–zirconia ceramics. *Br. Ceram. Trans. J.*, 1993, **85**, 156–160.
13. Kingery, W. D., Bowen, H. K. and Uhlmann, D. R., *Introduction to Ceramics*. John Wiley and Sons, New York, 1976.
14. Cho, J., Rickman, J. M., Chan, H. M. and Harmer, M. P., Modeling of grain boundary segregation behavior in aluminum oxide. *J. Am. Ceram. Soc.*, 2000, **83**, 344–352.
15. Cawley, J. D. and Halloran, J. W., Dopant distribution in nominally yttrium-doped sapphire. *J. Am. Ceram. Soc.*, 1986, **69**, 195–196.
16. Fang, J., Thompson, A. M., Harmer, M. P. and Chan, H. M., Effect of yttrium and lanthanum on the final-stage sintering behavior of ultrahigh-purity alumina. *J. Am. Ceram. Soc.*, 1997, **80**, 2005–2012.
17. Kibbel, B. W. and Heuer, A. H., Ripening of inter- and intragranular ZrO_2 particles in ZrO_2-toughened Al_2O_3. In *Advances in Ceramics,* Vol 12, ed. N. Claussen, M. Ruhle and A. H. Heuer. Am. Ceram. Soc., Columbus, USA, 1984, pp. 415–424.
18. Westmacott, K. H., Fountain, C. W. and Stirton, R. J., On the spacing of dispersed obstacles. *Acta Metall.*, 1966, **14**, 1628–1629.
19. Kocks, U. F., On the spacing of dispersed obstacles. *Acta Metall.*, 1966, **14**, 1629–1631.
20. Morrell, R., *Handbook of Properties of Technical & Engineering Ceramics, Part 1, An Introduction for the Engineer and Designer*. HMSO, London, UK, 1985.
21. Spriggs, R. M. and Vasilos, T., Effect of grain size on transverse bend strength of alumina and magnesia. *J. Am. Ceram. Soc.*, 1963, **46**, 224–228.
22. Tuan, W. H. and Kuo, J. C., Contribution of residual stress to the strength of abrasive ground alumina. *J. Eur. Ceram. Soc.*, 1999, **19**, 1593–1597.
23. Becher, P. F., Toughening behaviour in ceramics associated with the transformation of tetragonal ZrO_2. *Acta Metall.*, 1986, **34**, 1885–1891.